Power System Design Optimization for a Ferry Using Hybrid-Shaft Generators

Thant Zin Oo, Yan Ren, Adams Wai-Kin Kong, Yi Wang, and Xiong Liu

***Abstract*—Ferry contributing a significant amount of greenhouse gas is one of the critical vessels to be electrified. Designing a power system for a ferry with hybrid-shaft generators is different from designing a power system for other vessels because of its fixed route. More clearly, ferries repeatedly travel between their port of origin and port of destination, and before the next voyage, the battery must be recharged to the initial state so that the optimal energy management scheme can be repeatedly applied. Furthermore, the flexibility of hybrid-shaft generators, which allow more fuel saving, increases design complexity. In this paper, a mixed-integer non-linear programming problem is first formulated, and a power management algorithm with an *initialization* step for fulfilling the battery recharging requirement and a *refinement* step for minimizing the fuel consumption is proposed. The simulation results obtained from data of an actual ferry show that the proposed power management algorithm can fully recharge the battery and consumes less fuel than a rule-based power management scheme. Simulations also reveal that fuel consumption depends on available shore power, highlighting the necessity to develop charging infrastructure for practical electrification. Because of its speed, the algorithm can support hardware sizing, e.g., battery sizing.**

***Index Terms*—Marine vehicles, Power systems, Energy Storage, Optimization methods, Marine Vehicle propulsion, Generators**

I. Introduction

According to the World Trade Organization and the International Maritime Organization, the maritime trade accounts for roughly 70% by value and 80% by volume of the global trade [1], [2] and emits 3% of global greenhouse gas [1]. As the world is now moving towards sustainable transport, the maritime shipping industry is also moving towards decarbonization [1], [3]. However, it affects a wide range of stakeholders from policymakers, shipping companies, and shipyards down to local entrepreneurs and consumers. Maritime shipping is critical for the global trade, which improves the standard of living for many people by lowering the costs of goods. The plan to decarbonize the shipping industry presents us with an economic and technical challenge that can be solved through design and engineering.

The maritime industry has been looking at electrification to increase efficiency and reduce the life-cycle cost of vessels [1]. Meanwhile, several technology developments bring a possible path towards a solution for decarbonizing the maritime industry. First, recent advances in battery technology in the automotive industry have been pushing the batteries prices down making the energy storage systems (ESSs) economically viable. And if this trend continues, the battery price is expected to fall below 100 US$/kWh in 2024 [4], and the lifecycle of battery has been significantly improved (90% of capacity remaining after 4500 full charging/discharging cycles) [5]. Second, the recent advances in Artificial Intelligence (AI) have enabled many industries to streamline their design processes and solve constrained optimization problems such as decarbonization effectively.

Although the battery price is falling, current energy density ($\approx$ 300 Wh/kg) of batteries cannot be scaled up to high-power maritime applications ($\approx 12,000$ Wh/kg for a 18,000-container vessel for a long-haul cargo route) [6], [7]. The seven largest maritime ferry networks in the world combined carry 109.53 million passengers annually accounting for a significant portion of greenhouse emission of the maritime industry ($\approx$ 0.12 kg per passenger-kilometer per ferry) [8]. These existing routes operate over 140 vessels, which are expected to be replaced in the near future, and approximately US$ 1.29 billion in investment is projected towards new vessels and facilities [8], [9]. As such, ferry is chosen as a case study for this research project.

Ferry, which has a fixed route, repeatedly traveling between the port of origin and the port of destination, is different from many other vessels, e.g., yacht. As with a ferry with a diesel power system, to electrify the ferry, its battery must be recharged to the initial state before the next voyage such that the optimal power management scheme can be repeatedly applied. Existing industry simulation tools, such as GT-suite [10], performing time-transient simulations for the chosen combination of power system components, require hours in each simulation and cannot guarantee a fully recharged energy storage at the end of each voyage. In the early stage of power system design for a vessel, the design engineers have to explore many combinations of power system components, which is very time-consuming especially for the Hybrid-Shaft Generators (HSGs) due to its two-way power flow and mechanical engineering constraints. The industry needs a simulation tool that can rapidly simulate a chosen combination of power system components and outputs the best operation strategy of the combination. Hence, this research aims to create a tool for marine power system design incorporating power system component modeling and optimization algorithms. The goal is to develop a rapid simulation tool to (1) guarantee a fully recharged ESS after each voyage, and (2) minimize fuel consumption for the ferry with HSGs. Because of the rapid

T. Z. Oo, Y. Ren and A.W.K. Kong are with Rolls-Royce Corporate Lab at Nanyang Technological University, Singapore. (email: {zinoo.thant, yan.ren, adamskong}@ntu.edu.sg). Y. Wang is with Rolls-Royce Singapore. (email: yi.wang4@rolls-royce.com). X. Liu is with the Energy Electricity Research Center, International Energy College, Jinan University, Zhuhai, China. (email: liushawn123@ieee.org). His contribution was done when he worked for Rolls-Royce Singapore.

simulation, the tool can handle hardware sizing, e.g., battery sizing. The proposed tool is expected to reduce greenhouse gas emissions while maintaining economic and operational efficiency.

A. Related Works

Technologies and practices used in land-based applications have been adopted in maritime applications [11], [12]. Components such as energy storage systems (ESS) and variable frequency drives have seen more widespread adoption in recent years. Similarly, new practices such as unit commitment, power system dispatch, and demand-side management have also been adopted by the industry [13]–[15].

Most importantly, a lot of studies have been done on marine power management using a variety of optimization and control techniques for all-electric ships with an integrated ESS. Kanellos et al. [13], [14] applied dynamic programming for demand side management and power generation schedule. In [15], Kanellos et al. used fuzzy control for power management. Sciberras et al. [16] proposed a stochastic approach for the power management system of a ferry with four medium-sized engines for an *all-electric* vessel. In [17], Scribberas et al. considered a *hybrid-electric* vessel and proposed a power management system based on particle swarm optimization, which belongs to evolutionary computing and seeks for near-global optimum. Shang et al. [18], [19] used the non-dominated sorting genetic algorithm II (NSGA-II) in the power management system to schedule power generation and reduce the greenhouse gas (GHG) emissions. Fang et al. [20], [21] proposed a two-step multi-objective optimization method to solve the joint power generation and voyage scheduling. In [22], Skjong et al. used Mixed-Integer Linear Programming (MILP) to find the optimal loading for engines.

All the above-mentioned works did not consider the ESS recharging requirement from the ferry. This requirement is named *energy balance* in this paper. Note that power balance and energy balance are different types of requirements. Power balance considers power supply and power demand at a particular time point, but energy balance (i.e., recharging the battery back to initial state) depends on the whole voyage, which constitutes a sequence of tasks and decisions, where earlier decisions would affect the later ones. Further, all the above-mentioned works except for [17] are for *all-electric* vessels, i.e., the mechanical power from engines is converted into electricity which is consequently converted back to mechanical power for propulsion as shown in Fig. 1b. Although all-electric architecture greatly simplifies the power management problem, the overall system efficiency is lowered partially because of the two energy conversions. Hybrid-electric architecture, which utilizes Hybrid Shaft Generators (HSGs) [23], [24] provides higher efficiency. In an HSG, the engine output shaft is connected to a three-way gearbox as shown in Fig.1a. Hence,

1) each propulsion load can be supplied by the engine or the electric bus or both, and
2) each main engine can supply power both to the propulsion load and electrical load.

This flexibility leads to more operational choices for effective power management but increases complexity of the problem.

Only a few works focused on the power system component selection, also known as, *hardware sizing*. Yan et al. [25] used particle swarm optimization to size and place ESS on navy ships with the goal of ship survivability. Mashayeka et al. [26] studied the sizing of energy storage for an electric ship where they formulated a dynamic optimization problem to find the optimal loading strategy for the ship generators. Boveri et al. [27] studied optimal sizing of an ESS for a vessel where they considered the lifecycle cost for different battery sizes. However, these works only considered linear loss function in battery charging and discharging which simplifies the problem. The proposed tool uses a non-linear loss function in battery charging and discharging to reflect the real-world application and focuses on battery sizing for selected engines and their corresponding components. The goal of this study is to enable a designer to estimate the OPEX cost of each architecture. However, CAPEX estimation is out of the scope of this paper and requires a component/hardware library and an associated dataset which is usually proprietary.

B. Contributions

The contributions of this paper are as follows:

- First, to reflect the real-world mechanical and electrical engineering constraints, non-linear loss functions are used to model engines, electric machines, and ESS (battery). Then, a mixed-integer non-linear programming (MINLP) problem is formulated for the power management module with *energy balance* and *power balance* constraints.
- Next, the formulated MINLP problem is *NP-hard*, and hence, decomposed into two tractable sub-problems: (i) battery discharging and charging to guarantee *energy balance*, and (ii) generator and shore power allocation to minimize the fuel consumption.
- A novel power management algorithm is proposed to ensure the battery *energy balance* in the *initialization* step and minimize the fuel consumption in the *refinement* step, which is composed of: (i) an Earth-mover's distance-inspired method for battery management, and (ii) an interior-point method for generator power dispatch.
- Extensive simulations were performed on three architectures (hybrid-electric, all-electric, and diesel-mechanical architectures) with the same ferry study case. Simulation results show that compared with a rule-based power management method, the proposed method generates lower fuel consumption results, guarantees the battery energy balance, and shows its potential in battery sizing. Furthermore, the simulation results also reveal the importance of charging infrastructure for electric ships.

The rest of the paper is organized as follows: Section II describes the system model and Section III presents the the problem formulation. Section IV describes the proposed algorithm, and Section V discusses the case study and the simulation results. Section VI concludes this paper.

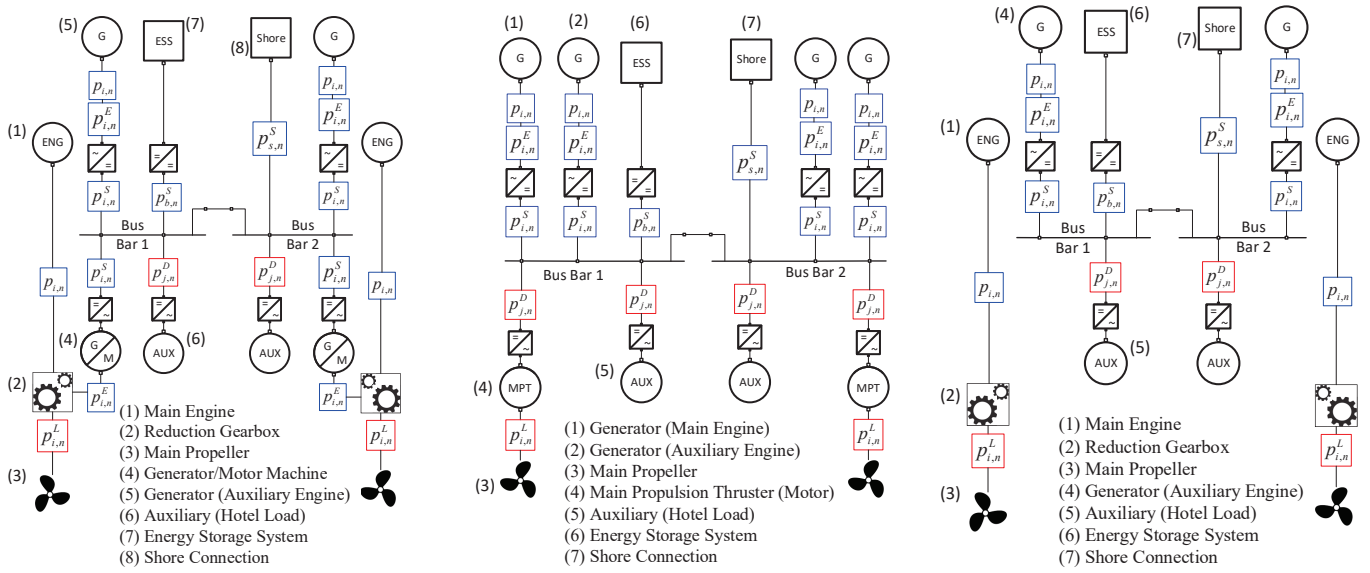

(a) Hybrid-electric architecture (b) All-electric architecture (c) Diesel-mechanical architecture

Fig. 1: Three DC bus power system architectures considered with 2 main engines, 2 auxiliary engines, and an energy storage system. The notations in the figure are defined in Table I.

II. System Model

A. Vessel Architecture

Consider a DC-bus architecture for the vessel micro-grid, as shown in Fig. 1a. The two main engines are configured as hybrid-shaft generators (HSG). Each propeller is mechanically connected to a main engine and an electrical generator/motor via a three-way reduction gearbox. Hence, the propeller can draw power from the engine, the electrical bus, or both sources simultaneously. Thus, each HSG (the entire assembly of the propeller, the main engine, and the generator/motor) can either be a power supply or a power demand. On the other hand, the two auxiliary engines (AEs) are configured as diesel generators (DG), which supply electrical power to the bus. For the Energy Storage System (ESS), a single battery pack is connected to the bus via a DC to DC converter. Note that the battery is a power supply while it is discharging and a power demand while it is charging. Furthermore, the vessel has a shore connection as an external power supply when it is available at the harbor.

Power demand can be divided into *propulsion* loads and *hotel* loads (including station-keeping thrusters, motors, and winches). In all the power system architectures, the *hotel* loads are supplied from the electrical bus. Their difference lies in how each power system architecture supplies the *propulsion* loads by mechanical power or electrical power or both. In the classical diesel-mechanical architecture as shown in Fig. 1c, each main engine (ME) solely supplies mechanical power to a propeller. For all-electric architecture, both main engines (MEs) are configured as DGs to generate electrical power for supplying *propulsion* and *hotel* loads. In the hybrid-electric architecture, each propeller can be supplied with mechanical power from the ME or the electrical power from the electrical bus or both, as shown in Fig. 1a.

Consider a vessel with J power demand loads, consisting of propulsion and hotel loads, and K power supplies, consisting of main engines, auxiliary engines, energy storage systems (ESS) and shore supply. In this study, it is assumed that load profiles of all N operational tasks are given, for example, at rest, acceleration, voyage, station-keeping, anchored, at port, etc. The n-th operational task refers to the n-th time interval (or time slot) where the power demand remains constant for the time interval. This sequence of operational tasks (or time slots) comprises an entire ferry cycle from the embarkation of cargo and passengers on one trip to embarkation on another trip. Note that the main engine speed remains constant during each operational task for *hybrid-electric* and *diesel-mechanical*, and the length of time intervals may vary depending on the operational tasks.

B. Power Balance

In a vehicular micro-grid, as in any other electrical system, the total power supply must always equal the total power demand at any time, i.e.,

$$\sum_j p^D_{j,n} = \sum_k p^S_{k,n}, \quad \forall n \in \mathcal{N}, \tag{1}$$

where $p^D_{j,n}$ denotes the power demand of the j-th load, and $p^S_{k,n}$ denotes the power supply of the k-th source at the n-th time slot.

Power demand includes all the loads and the losses on the demand side. Let $p^L_{j,n}$ be the power demand of the j-th load and $h_j(p^L_{j,n})$ be its corresponding power loss. Thus, the total power demand at the bus is

$$\sum_j p^D_{j,n} = \sum_j \left(p^L_{j,n} + h_j(p^L_{j,n})\right), \quad \forall n \in \mathcal{N}, \tag{2}$$

where $h_j(\cdot)$ is the load specific non-linear loss function, which depends on the type of load, e.g., electrical machine or hotel. Note that the load does not include the propeller

TABLE I: Table of Notations

Symbol	Domain	Unit	Description
n	$\in \mathbb{Z}$		Time instance or task index
i	$\in \mathbb{Z}$		Supply branch index on electrical bus
j	$\in \mathbb{Z}$		Demand branch index on electrical bus
Δt_n	$\in \mathbb{R}^+$	s	Time duration (time slot length) of the n-th task
$p^L_{j,n}$	$\in \mathbb{R}^+$	W	Electrical power demand by the j-th load
$p^D_{j,n}$	$\in \mathbb{R}^+$	W	Electrical power demand on the bus (load + loss)
$x_{i,n}$	$\in \{0,1\}$		Switch on/off for i-th HSG or DG
$p_{i,n}$	$\in \mathbb{R}^+$	W	Mechanical power generated (+ive) by the i-th HSG or DG
$p^L_{i,n}$	$\in \mathbb{R}^+$	W	Mechanical power demand by the i-th HSG/propeller
$p^E_{i,n}$	$\in \mathbb{R}$	W	Electrical power supplied (+ive) to/ drawn (-ive) from the bus by HSG/DG
$p^S_{i,n}$	$\in \mathbb{R}$	W	Electrical power supply (positive)/demand (negative) on bus by HSG/DG
$F_{i,n}$	$\in \mathbb{R}^+$	kg/h	Fuel consumption by the i-th HSG/DG
$p_{b,n}$	$\in \mathbb{R}$	W	Battery discharging (+ive) / charging (-ive) power
$p^S_{b,n}$	$\in \mathbb{R}$	W	Electrical power supply (positive)/demand (negative) on bus by battery
Q^{rated}	$\in \mathbb{R}^+$	Wh	Battery capacity
Q_n	$\in \mathbb{R}^+$	Wh	Amount of energy stored in battery
$\widetilde{Q}_n$	$\in [0,1]$		Battery State of Charge (SOC), i.e., normalized stored energy
q_n	$\in \mathbb{R}$	Wh	Battery discharging (+ive) / charging (-ive) energy
$p^S_{s,n}$	$\in \mathbb{R}^+$	W	Electrical power supply on bus by shore
P_n	$\in \mathbb{R}$	W	Electrical power surplus (+ive)/ deficit (-ive) at the bus
$g_i(\cdot)$			Generator specific loss function for power loss in generation
$g_b(\cdot)$			Battery specific loss function for discharging / charging
$h_j(\cdot)$			Load specific loss function for power loss in load

loads connecting to the Hybrid Shaft Generators (HSGs) or the battery (ESS) charging loads. HSG and battery can either be power suppliers or power consumers. In this paper, they are included in the power supply side.

In contrast, the power supply includes generators, battery, shore power, and the losses of the supply side. Hence, the total power supply at the bus can be broken down as follows:

$$\sum_k p^S_{k,n} = p^S_{b,n} + p^S_{s,n} + \sum_i x_{i,n} \cdot p^S_{i,n} \quad \forall n \in \mathcal{N}. \tag{3}$$

in which $x_{i,n} \in \{0,1\}$ indicates whether the i-th generator is switched on or off, $\sum_i x_{i,n} \cdot p^S_{i,n}$ represents the power supplied by the generators, $p^S_{b,n}$ represents the battery power at the bus, and $p^S_{s,n}$ represents the shore power at the bus.

Substituting, (3) in (1), the power balance constraint equation is obtained, i.e.,

$$p^S_{b,n} + p^S_{s,n} + \sum_i x_{i,n} \cdot p^S_{i,n} - \sum_j p^D_{j,n} = 0, \quad \forall n \in \mathcal{N}. \tag{4}$$

C. Generators

The generator power supplied to the bus $p^S_{i,n}$ consists of:

$$p^S_{i,n} = p^E_{i,n} - g_i(p^E_{i,n}), \quad \forall n \in \mathcal{N} \tag{5}$$

where $p^E_{i,n}$ represents the electric power supplied to the bus by the generators and $g_i(\cdot)$ is the source-specific non-linear loss function, which depends on generator type. Since the load and power of HSG are incorporated into a single branch, $p^S_{i,n}$ indicates either the power supplied to the bus or power drawn from the bus.

The relationship between the electric power $p^E_{i,n}$ and the mechanical power supplied by the generators can be represented as follows [23], [24]:

$$p^E_{i,n} = \begin{cases} (1-\eta_i)p_{i,n} - p^L_{i,n}, & \text{for HSG.} \\ p_{i,n}, & \text{for DG.} \end{cases} \tag{6}$$

For the HSG, the electric power equals the power generated by the generator at the source $p_{i,n}$ minus the load demand of the i-th propeller $p^L_{i,n}$ at the n-th task with considering the mechanical power loss η_i in the reduction gearbox. For diesel generator (DG), the electric power directly equals the power generated by the DGs $p_{i,n}$. Both HSG and DG power is limited in a range based on actual components available on the market:

$$p_{i,n} \in [p^{\min}_{i,n}, p^{\max}_{i,n}]. \tag{7}$$

Furthermore, the power supplied and drawn by HSG is limited mechanically by the available electric machine, i.e.,

$$p^E_{i,n} \in [-p^{\text{threshold}}_{\text{HSG}}, p^{\text{threshold}}_{\text{HSG}}]. \tag{8}$$

Note that when power is supplied to the bus, $p^S_{i,n} \geq 0$, and $p^E_{i,n} \geq 0$, whereas when power is drawn from the bus, $p^S_{i,n} < 0$, and $p^E_{i,n} < 0$.

The fuel consumption (FC) by the i-th generator for the n-th task outputting $p_{i,n}$ can be calculated as:

$$F_{i,n} = x_{i,n} \cdot f_i(p_{i,n}), \quad \forall n \in \mathcal{N} \tag{9}$$

where $f_i(\cdot)$ is a generator-specific dynamic fuel consumption function.

D. Shore Connection

The shore power supplied to the bus is defined as:

$$p^S_{s,n} = p_{s,n} \in [0, p^{\max}_{s,n}] \tag{10}$$

where $p_{s,n}$ represents the shore power at the source and $p^{\max}_{s,n}$ is the maximum shore power supply.

E. Energy Storage System or Battery

The battery power imparted to the bus can either be a supply (discharging) or a demand (charging) on the bus:

$$p^S_{b,n} = p_{b,n} \in [-p_b^{\text{charge}}, p_b^{\text{discharge}}], \quad \forall n \in \mathcal{N} \tag{11}$$

where $p_{b,n}$ represents the discharging/charging power at the battery and the range of the battery power is limited by the maximum discharging power, $p_b^{\text{discharge}}$, and the maximum charging power, $-p_b^{\text{charge}}$, of the battery.

The corresponding change in energy due to charging or discharging can be calculated as:

$$q_n = \Delta t_n \cdot p^S_{b,n} + g_b(\Delta t_n \cdot p^S_{b,n}), \quad \forall n \in \mathcal{N} \tag{12}$$

$$q_n \in [-q^{\text{charge}}, q^{\text{discharge}}] \tag{13}$$

in which q_n is the battery discharging/charging energy on the bus, $g_b(\cdot)$ is the battery-specific non-linear loss function, and Δt_n is the time duration of the n-th task. Note that, by sign convention, $p^S_{b,n} \geq 0, p_{b,n} \geq 0$, when the battery is discharging, and, $p^S_{b,n} < 0, p_{b,n} < 0$, when the battery is charging.

Then, the energy stored inside the battery is updated as:

$$Q_{n+1} = Q_n + q_n \tag{14}$$

$$Q_m = Q_0 + \textstyle\sum_{n=0}^{m-1} q_n \tag{15}$$

where Q_0 represents the initial state of battery energy, and Q_m represents the m-th state of battery energy. To extend the battery life, the amount of energy stored in the battery at each task/time-instance is limited to a range:

$$Q_n \in [Q^{\min}, Q^{\max}], \quad \forall n \in \mathcal{N} \tag{16}$$

where $Q^{\min}$ and $Q^{\max}$ correspond to the lower and upper limit of the energy stored inside the battery. The state of charge (SOC) of the battery is the normalized stored energy in battery, i.e.,

$$\widetilde{Q}_n = Q_n / Q^{\text{cap}}, \quad \forall n \in \mathcal{N}. \tag{17}$$

where Q^{cap} denotes the battery capacity, and $\widetilde{Q}_n$ denotes SOC of battery with lower and upper bounds given as $\widetilde{Q}_n \in [0.1, 0.9]$ as an industry rule of thumb.

F. Energy Balance at the Battery

To achieve electrification in the maritime industry, the battery discharging and charging cycle must be carefully considered. Ferry generally has a fixed route and scheduled port calls. Hence, the sequence of tasks (a voyage or cycle) is repeated periodically. Hence, the battery state of charge (SOC) should be the same at the beginning and end of each cycle. Hence, a constraint called energy balance is added which states the final SOC must equal the initial SOC, i.e., $Q_N = Q_0$. In other words,

$$\sum_{n=1}^{N} q_n = 0. \tag{18}$$

This constraint ensures that the discharged energy is fully recharged back at the end of N tasks.

III. Problem Formulation

Many works in the maritime industry have formulated their problems as multiple-objective optimization problems [13]–[21]. The objective functions include key performance indicators (KPIs) such as Energy Efficiency Operational Indicator (EEOI), greenhouse gas (GHG) emissions, and operational cost, which are functions of fuel consumption. Moreover, most KPIs depend on external factors; for instance, the operational cost depends on the fuel oil price, which is dynamically changing with global supply and demand. By optimizing the fundamental engineering indicator fuel consumption, the above KPIs are also optimized implicitly. Furthermore, the optimization problem is simplified, leading to an increase in computational efficiency. The design goal is to minimize the fuel consumption subject to the power balance constraint, the energy balance constraint, and the power limit constraints of the generators and battery. Hence, the problem can be modeled as:

$$\begin{aligned}
\underset{\boldsymbol{x},\boldsymbol{p},\boldsymbol{p}_s,\boldsymbol{q}}{\text{minimize:}} \quad & F = \textstyle\sum_n F_n = \sum_n \sum_i x_{i,n} \cdot f_i(p_{i,n}) \qquad \textbf{(P0)} \\
\text{subject to :} \quad & p^S_{b,n} + p^S_{s,n} + \textstyle\sum_i x_{i,n} \cdot p^S_{i,n} - \sum_j p^D_{j,n} = 0, \ \forall n \\
& \textstyle\sum_{n=1}^{N} q_n = 0. \\
& x_{i,n} \in \{0,1\}, \quad p_{i,n} \in [p^{\min}_{i,n}, p^{\max}_{i,n}], \\
& p_{s,n} \in [0, p^{\max}_{s,n}], \quad Q_n + q_n \in [Q^{\min}, Q^{\max}]
\end{aligned}$$

(P0) is a mixed-integer non-linear programming (MINLP) problem, which is combinatorial, non-convex and NP-hard [28]. Hence, for tractability, **(P0)** is decomposed into two sub-problems: the battery discharging and charging problem **(P1)**, and the generator and shore power allocation problem **(P2)**.

A. Battery Discharging and Charging Problem

If generator power, $(x_{i,n} \cdot p_{i,n}), \forall (i,n)$ and shore power, $p_{s,n}, \forall n$, are known, the battery charging/discharging energy amount can be found through the minimization below.

$$\begin{aligned}
\underset{\boldsymbol{q}}{\text{minimize:}} \quad & \left| p^S_{b,n} + p^S_{s,n} + \textstyle\sum_i x_{i,n} \cdot p^S_{i,n} - \sum_j p^D_{j,n} \right| \qquad \textbf{(P1)} \\
\text{subject to :} \quad & \textstyle\sum_{n=1}^{N} q_n = 0. \\
& Q_n + q_n \in [Q^{\min}, Q^{\max}]
\end{aligned}$$

where $|\cdot|$ is the L1-norm. Note that there is infinite number of linear combinations for battery energy allocation problem **(P1)** due to (18).

B. Generator and Shore Power Allocation Problem

If battery charging/discharging energy, $q_n, \forall n$, is known and fulfills the constraint (18), the generator and shore power for each time step n can be found as follows:

$$\begin{aligned} \underset{\boldsymbol{x},\boldsymbol{p},\boldsymbol{p}_s}{\text{minimize:}} \quad & F = \textstyle\sum_n F_n = \sum_n \sum_i x_{i,n} \cdot f_i(p_{i,n}) \qquad \textbf{(P2)} \\ \text{subject to :} \quad & p^S_{b,n} + p^S_{s,n} + \textstyle\sum_i x_{i,n} \cdot p^S_{i,n} - \sum_j p^D_{j,n} = 0, \ \forall n \\ & p_{i,n} \in [p^{\min}_{i,n}, p^{\max}_{i,n}], \quad p_{s,n} \in [0, p^{\max}_{s,n}] \end{aligned}$$

(P2) is still combinatorial and non-convex. Since the fuel consumption in the n-th task is independent from other tasks, **(P2)** can be further decomposed into N smaller sub-problems. Let $\boldsymbol{x}^*$, $\boldsymbol{p}^*$, $\boldsymbol{p}^*_s$ be the solution of **(P2)**, then

$$\begin{aligned} \{\boldsymbol{x}^*, \boldsymbol{p}^*, \boldsymbol{p}^*_s\} &= \arg\min F(\boldsymbol{x}, \boldsymbol{p}, \boldsymbol{p}_s) \qquad (19) \\ &= \arg\min \textstyle\sum_n F_n(\boldsymbol{x}_n, \boldsymbol{p}_n, \boldsymbol{p}_{s,n}) \\ \{\boldsymbol{x}^*_n, \boldsymbol{p}^*_n, \boldsymbol{p}^*_{s,n}\} &= \arg\min F_n(\boldsymbol{x}_n, \boldsymbol{p}_n, \boldsymbol{p}_{s,n}). \qquad (20) \end{aligned}$$

In maritime application, a vessel usually has only a few generators. Moreover, the generators are installed in symmetric pairs (i.e., the same model for port and starboard sides). Hence, if a vessel has 4 generator installed as shown in Fig. 1, $\boldsymbol{x}_n$ has $2^{(4-1)} + 1 = 9$ possible combinations for the n-th task, i.e.,

$$\boldsymbol{x}_n \in \begin{Bmatrix} 0 & 1 & 0 & 1 & 1 & 0 & 1 & 1 & 1 \\ 0 & 0 & 0 & 1 & 0 & 0 & 1 & 0 & 1 \\ 0 & 0 & 1 & 0 & 1 & 1 & 1 & 1 & 1 \\ 0 & 0 & 0 & 0 & 0 & 1 & 0 & 1 & 1 \end{Bmatrix}, \quad \forall n \in \mathcal{N}. \quad (21)$$

More combinations can further be ruled out by checking the lower and upper bounds, i.e.,

$$\sum_i x_{i,n} \cdot p^{\min}_{i,n} \leq \sum_j p^D_{j,n} - p^S_{b,n} - p^S_{s,n} \leq \sum_i x_{i,n} \cdot p^{\max}_{i,n} \quad (22)$$

Thus, the fuel consumption can be exhaustively computed for all feasible combinations of $\boldsymbol{x}_n$. Solving (**P3**) yields the optimal generator $\boldsymbol{p}^*_n$ and shore power $\boldsymbol{p}^*_{n,s}$ for the n-th task and a combination $\boldsymbol{x}_n$.

$$\begin{aligned} \underset{\boldsymbol{p}_n,\boldsymbol{p}_{s,n}}{\text{minimize:}} \quad & F_n = \textstyle\sum_i f_i(p_{i,n}) \qquad \textbf{(P3)} \\ \text{subject to :} \quad & p^S_{b,n} + p^S_{s,n} + \textstyle\sum_i p^S_{i,n} - \sum_j p^D_{j,n} = 0, \ \forall n \\ & p_{i,n} \in [p^{\min}_{i,n}, p^{\max}_{i,n}], \quad p_{s,n} \in [0, p^{\max}_{s,n}] \end{aligned}$$

The convexity of **(P3)** depends on the fuel consumption function, $f_i(\cdot)$, and the non-linear loss functions, $g_i(\cdot)$ [28]. For this study, **(P3)** is non-convex and non-linear and *interior-point* method is used to solve it [29]. Algorithm 1 describes how **(P2)** is solved via solving N smaller sub-problems.

IV. Power Management Algorithm

The proposed power management algorithm is composed of two main steps: *initialization* and *refinement*. Each step consists of two components *battery update* and *engine update*. The initialization step aims at finding an initial solution which satisfies both power balance (4) and energy balance (18) based on the load profile. In contrast, the refinement step focuses on the minimization of fuel consumption through moving and balancing the battery energy.

Algorithm 1: Engine Update

Input: $\forall n,\ p^D_{j,n},\ p^S_{b,n},\ p^S_{s,n} = p^{S,\max}_{s,n}$
1: Find all possible combinations $\boldsymbol{x}_n \in \mathcal{X}$ using (21)
2: Find feasible combinations using (22), i.e., $\mathcal{X}^f \subseteq \mathcal{X}$
3: **for** $\boldsymbol{x}_n \in \mathcal{X}^f$ **do**
4: Solve **(P3)** using *interior-point* method.
5: Find $\boldsymbol{x}^*_n = \arg\min F_n(\boldsymbol{x}_n, \boldsymbol{p}^*_n, \boldsymbol{p}^*_{s,n})$ from $\mathcal{X}^f$.
Output: $\forall (n,i),\ x^*_{i,n},\ p^*_{i,n},\ p^{S,*}_{s,n}$

Algorithm 2: Initialization Procedure

Input: $\forall n, i,\ p^S_{i,n} = p^{S,\max}_{i,n},\ p^S_{s,n} = p^{S,\max}_{s,n},\ p^S_{b,n} = 0$
1: Initialize deficit and surplus power P_n
2: Choose time step with the highest deficiency t_n. Discharge battery to fill deficiency
3: Update battery power: $\hat{p}^S_{b,n} = p^S_{b,n} + \Delta p_{b,n} > 0$
4: Choose another time step with the lowest battery charging power and recharge battery to meet energy balance (18).
5: Update battery power: $\hat{p}^S_{b,m} = p^S_{b,m} + \Delta p_{b,m} < 0$.
6: Update battery voltage and SOC
7: Update power deficit and surplus P_n
8: **if** *Power deficit exists for any* n **then**
9: Go back to Line 2.
10: Minimize fuel consumption with fixed battery power $p^S_{b,n}$: Algorithm 1.
Output: $\forall n, i, p^{S,*}_{i,n},\ p^{S,*}_{s,n},\ p^{S,*}_{b,n}$

A. Initialization Procedure

Knowing that the solution for **(P1)** is not unique, a feasible solution for **(P1)** is first sought. The generator power and shore power are set to their respective boundary values, i.e., $x_{i,n} = 1$, $p_{i,n} = p^{\min}_{i,n}, \forall n$ and $p_{s,n} = p^{\max}_{s,n}$. Note that the maximum shore power, $p^{\max}_{s,n} = 0$ during voyage and at harbor without shore connection. Similarly, the maximum generator power output, $p^{\max}_{i,n} = 0$, at harbor reflects emission control without introducing a separate additional emission constraint.

First, power deficit or surplus of the generator and shore power are calculated. At time index n, based on the load demand on the bus $\sum_j p^D_{j,n}$, the deficit and surplus power P_n of the generators can be defined as:

$$P_n = p^S_{b,n} + p^{S,\max}_{s,n} + \sum_i x_{i,n} \cdot p^{S,\min}_{i,n} - \sum_j p^D_{j,n} \qquad (23)$$

If $P_n > 0$, power supply is larger than power demand (load plus loss) and there is power surplus; otherwise it is power deficit, except for $P_n = 0$. The major challenge is to always keep power balance, i.e., $P_n = 0$. Although the concept seems simple and trivial, the challenge lies in accurately modeling the non-linear loss functions: $h_j(\cdot)$, $g_i(\cdot)$, and $g_b(\cdot)$. Furthermore, the energy balance constraint (18) to recharge the battery adds additional complexity.

Let $P_n < 0$ represent the deficit power (23). After discharging battery power, the deficit power should be zero: $\widetilde{P}_n = 0$

(feasible and power balanced). Then,

$$\widetilde{P}_n = \tilde{p}^S_{b,n} + p^{S,\max}_{s,n} + \sum_i x_{i,n} \cdot p^{S,\min}_{i,n} - \sum_j p^D_{j,n}. \quad (24)$$

Subtracting (23) from (24) yields:

$$\widetilde{P}_n - P_n = \tilde{p}^S_{b,n} - p^S_{b,n} = \Delta p^S_{b,n} \quad (25)$$
$$\Delta p^S_{b,n} = -P_n, \quad \forall n,$$

where $\Delta p^S_{b,n}$ is the change in battery power to balance the demand and supply. Similarly, the change in battery power can be derived for power surplus, $P_n > 0$. Multiplying (25) with Δt_n on both sides, the change in amount of energy or energy exchange amount is obtained:

$$q_n = -\Delta t_n \, P_n, \quad \forall n. \quad (26)$$

From the energy balance (18), q_N is obtained, i.e.,

$$q_n = -\sum_{m \in \mathcal{N} \setminus \{n\}} q_m. \quad (27)$$

When the battery discharges q_n amount of energy at the n-th time slot, the battery can recharge at the m-th time slot where $m \in \{n+1, n+2, \ldots, N\}$. Since the initial SOC is assumed to be at maximum, i.e., $Q_0 = Q^{\max}$, the battery can only be re-charged after it is first discharged, i.e, $Q_m < Q^{\max}$, $\forall m > n$. For partial recharge scenario of the discharged energy q_n, the number of combinations further increases. Since it is not efficient to simultaneously compute all feasible discharging and charging solutions, a two element subset $\mathcal{N}_S = \{m, n\}$ is considered. Then, (27) becomes

$$\tilde{q}_n = -\tilde{q}_m \quad (28)$$

where the amount of energy discharge and recharged is calculated as:

$$\tilde{q}_n = -\tilde{q}_m = \min\{|q_n|, |q_m|\}. \quad (29)$$

Then, the battery can be iteratively recharged for discharged energy as follows:

$$q_n = \sum_k \tilde{q}_{k,n} = -\sum_{m \in \mathcal{N} \setminus \{n\}} \sum_k \tilde{q}_{k,m}. \quad (30)$$

where $\tilde{q}_{k,n}$ denotes a discharge at the n-th time slot at the k-th iteration. The charging solution ensures that energy balance constraint (18) is satisfied. Note that the amount of energy discharged and recharged, q_n, must be within the battery discharge/charge limits, i.e., constraint (13), and the SOC of the battery must be within its limits, i.e., constraint (16). Detailed procedure is given in Algorithm 2.

At the first iteration, the battery power is set to zero, i.e., $p^S_{b,n} = 0$, while the generator and shore power are set to maximum. Thus, P_n reflects the deficit and surplus power of generators and shore connection when switching off the battery. For the surplus conditions, $P_n > 0$, the generator and shore power are sufficient enough for the load demand and losses. It means that the power balance at time index n is ready to be met. When $P_n < 0$, the generator and shore power are not enough to supply the load demand and losses and there is power deficit. The battery needs to discharge power $p^S_{b,n} > 0$ to meet the power balance at n. However, to keep the energy balance, after battery power (energy) discharge at n, the battery needs to be charged back in another time index m with the surplus condition, i.e., $-p^S_{b,m} \cdot \Delta t_m \geq p^S_{b,n} \cdot \Delta t_n$. Please note that the power balance at time index n might not be met at once due to the limit of surplus power at m. Thus the battery energy allocation process would be repeated until the power deficit is met.

At the beginning, the deficit power is sorted in a descending order (from high to low). The time step with a higher deficiency has a higher priority to be filled with battery discharging. The time step with a higher energy surplus has a higher priority for the battery to recharge to meet energy balance. After the assignment of battery discharging and charging power/energy, the deficit and surplus power would be updated until no deficiency condition exists, $P_n >= 0$, $\forall n \in \mathcal{N}$. After the battery has filled all the power deficits, the battery power $p^{S,*}_{b,n}$ is fixed and the power from generators and shore with surplus are reduced such that all $P_n = 0$ using Algorithm 1.

Algorithm 3: Refinement Procedure

Input: Output from Alg.2: $\forall n, i, p^{S,*}_{i,n}$, $p^{S,*}_{s,n}$, $p^{S,*}_{b,n}$, $\Delta q_n = p^{S,\max}_{b,n}$, $q_{step} > 0$

1: For all $n, m \leq N$, $n \neq m$, calculate $\Delta F_{n,m}$
2: Find the maximum fuel consumption reduction, i.e., for a given Δq, find n^* and m^* that have the lowest $\Delta F_{n^*,m^*}$.
3: **if** $\Delta F_{n^*,m^*} < 0$ **then**
4: Update battery at time steps n^* and m^*.
5: Update the SOC/battery energy and battery voltage.
6: Update the generator using Algorithm 1,
7: Update shore power.
8: Go back to Line 1.
9: **else**
10: Update $\Delta q_n = \Delta q_n - q_{step}$, $q_n + \Delta q_n \in \{-q^{\text{charge}}, q^{\text{charge}}\}$.
11: **if** $\Delta q_n \leq -Q^{\max}$ **then**
12: Go back to Line 1.

Output: $\forall n, i, p^{S,**}_{i,n}$, $p^{S,**}_{s,n}$, $p^{S,**}_{b,n}$

B. Refinement Procedure

The refinement step, which is inspired by the Earth-mover's distance, aims at minimizing the fuel consumption with the output of the initialization step as input. The results of the initialization step, including battery, generator, and shore control logic are both power-balanced and energy-balanced. For energy balance, it means that $\sum_{n \in \mathcal{N}} q_n = 0$, where q_n represents the energy changed in the battery at n. Then, if a small amount of energy Δq_n is moved from one time step t_n to another time step t_m, the generator and shore power would be further adjusted. For instance, at time step t_n, an amount of energy $\Delta q_n > 0$ is discharged. To maintain the energy balance, the same amount of energy Δq_m should be charged back at another time step t_m:

$$\Delta q_n = -\Delta q_m, \quad n, m \in \mathcal{N}. \quad (31)$$

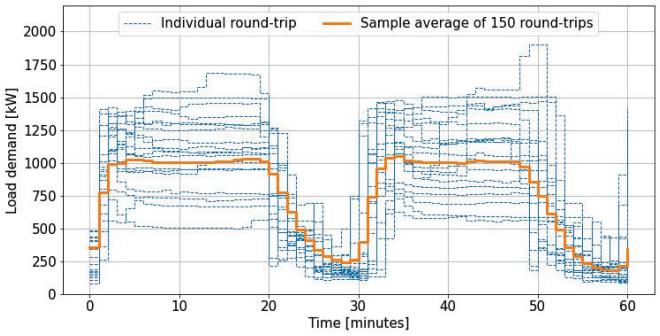

Fig. 2: Extracted load profile for simulation [22].

If $\Delta q_n > 0$, the battery would discharge energy at n and recharge energy at m. If $\Delta q_n \leq 0$, the battery would charge at n and discharge at m. Then the battery power at n and m can be updated as follows:

$$p^S_{b,n} + \Delta p_{b,n} = \frac{q_n + \Delta q_n}{\Delta t_n} \tag{32}$$

$$p^S_{b,m} + \Delta p_{b,m} = \frac{q_m - \Delta q_n}{\Delta t_m} \tag{33}$$

where $\Delta p_{b,n}$ and $\Delta p_{b,m}$ represent the change in battery power.

With the new battery power, the generator and shore power can be updated based on the power balance constraint using Algorithm 1:

$$\sum_i (p^S_{i,n} + \Delta p^S_{i,n}) + p^S_{s,n} + \Delta p^S_{s,n} = \sum_j p^D_{j,n} - p^S_{b,n}, \tag{34}$$

$$\sum_i (p^S_{i,m} + \Delta p^S_{i,m}) + p^S_{s,m} + \Delta p^S_{s,m} = \sum_j p^D_{j,m} - p^S_{b,m}, \tag{35}$$

where $\Delta p^S_{i,n}$ and $\Delta p^S_{i,m}$ represent the change of generator power at the bus, and $\Delta p^S_{s,n}$ and $\Delta p^S_{s,m}$ represent the change of shore power. Note that when the vessel is docked at the harbor, the generators are turned off to reduce emissions, i.e., $p^{\max}_{i,n} = 0$. Therefore, the refined fuel consumption based on the new generator power is:

$$F_n + \Delta F_n = \sum_i f_i \left(p_{i,n} + \Delta p_{i,n}\right), \tag{36}$$

$$F_m + \Delta F_m = \sum_i f_i \left(p_{i,m} + \Delta p_{i,m}\right), \tag{37}$$

where ΔF_n and ΔF_m represent the change of fuel consumption, and $\Delta p_{i,n}$ and $\Delta p_{i,m}$ represent the change of generator power with considering the loss. If $\Delta F_{n,m} = \Delta F_n + \Delta F_m < 0$, then the fuel consumption for time n and m is reduced. Thus, the fuel consumption is reduced iteratively through moving and balancing the battery energy. The refinement procedure is presented in Algorithm 3. Note that the refinement step for the reduction of fuel consumption is based on greedy search. Thus the final is a local optima.

V. Case Study

A ferry traveling back and forth between Port A and Port B is taken as a case study [22]. The average travel time is approximately 60 minutes for round-trip, excluding the time of the vessel docked at the harbor. The dataset contains power generated by each diesel-generator of an all-electric ferry [22] from 150 round-trips recorded in a period of 7 days. A load profile is extracted from the dataset by taking the sample mean for the case study, as shown in Fig 2. The battery specifications are referenced from [30]. Extensive simulations are performed and the simulation results of a ferry using the publicly available data from [22] are reported.

TABLE II: Vessel Configuration

Parameter/Component	Value/Rating (each)
2× Diesel engine (Main)	1200 kW
2× Diesel engine (Auxiliary)	640 kW
1× Energy storage (Battery)	0-500 kWh
1× Shore power supply (Harbor A)	0-500 kWh

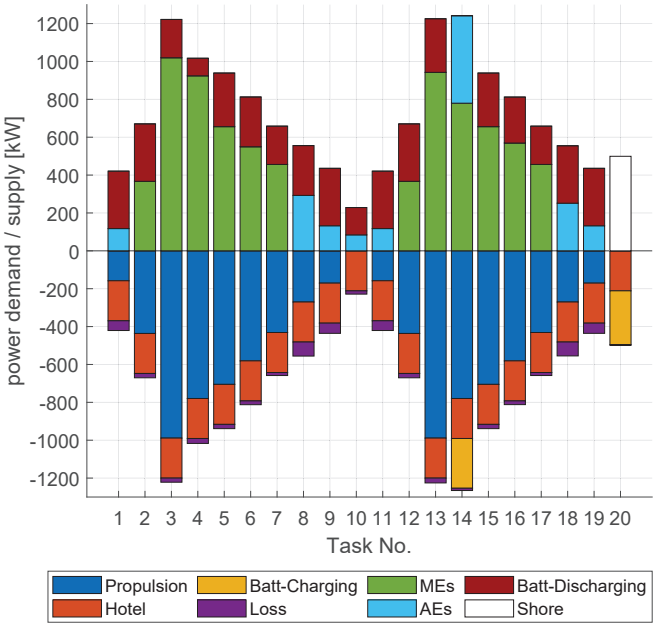

Fig. 3: Power demand (negative) and supply (positive) for round-trip load profile with 300 kWh battery with C-rate (discharge/charge) 2.2C/1.6C, and 500 kW shore power.

The vessel in this study uses a direct-current (DC) bus for electrical systems as shown in Fig. 1a. The rated powers of the major components and the experimental setup are given in Table II. For fuel consumption calculation, this case study uses the Specific Fuel Consumption (SFC) curves given in [22, Fig. 4], which shows that SFCs of the main engines, $f_1(\cdot)$ and $f_2(\cdot)$, are convex but SFCs of the auxiliary engines, $f_3(\cdot)$ and $f_4(\cdot)$ are non-convex. In our experiments, quadratic power loss is used, i.e., $g_i(p_i) = a_i p_i^2 + b_i p_i + c_i$, where a_i, b_i and c_i are constants ($c_i = 0$, $b_i = 0.98 \cdot 0.96$, $a_i = b_i^2/100$). Next, Matlab simulations are run to investigate the effect of battery size and shore power on fuel consumption (FC). Simulation time for each configuration takes approximately 6 minutes ($300 \sim 400$ seconds) which is significantly faster than the standard industry simulation tool such as GT-suite [10]. The FC results with varying battery size and shore power available are plotted in Figs. 3–4. The simulation results are compared

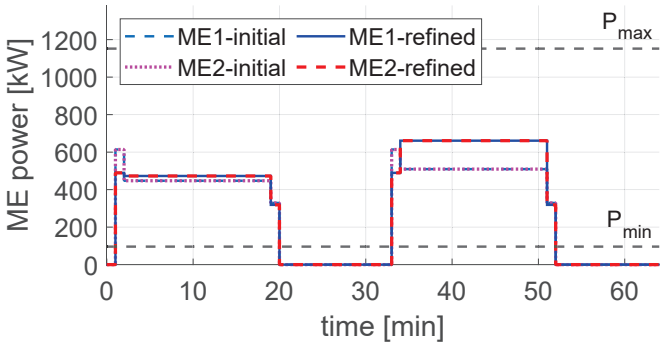

(a) Main engine (HSG) power

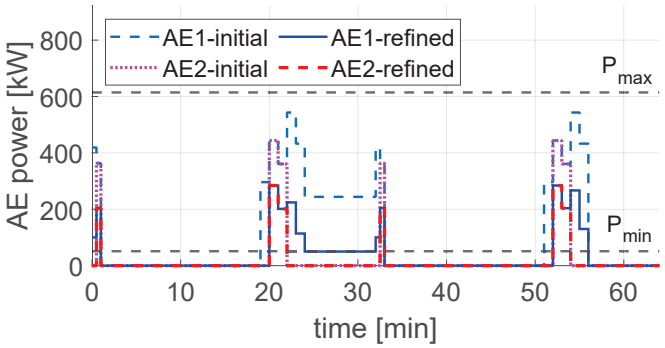

(b) Auxiliary engine (DG) power

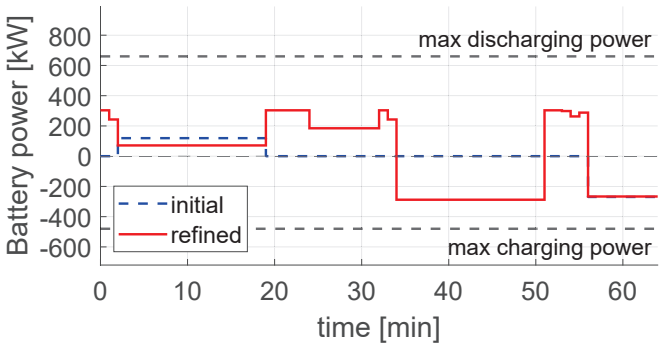

(c) Battery (ESS) power

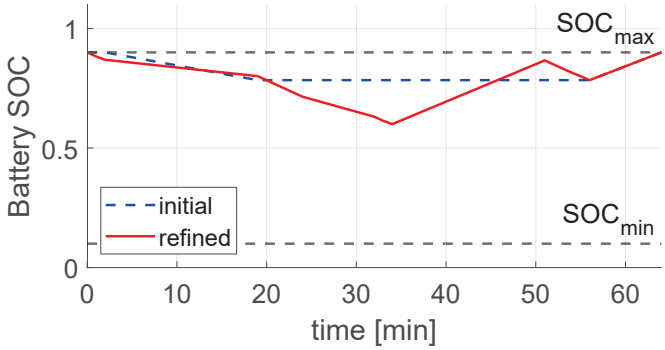

(d) Battery state of charge (SOC)

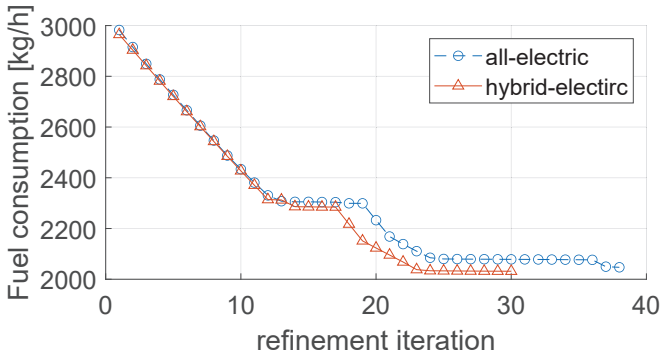

(e) Fuel consumption reduction in the refinement stage

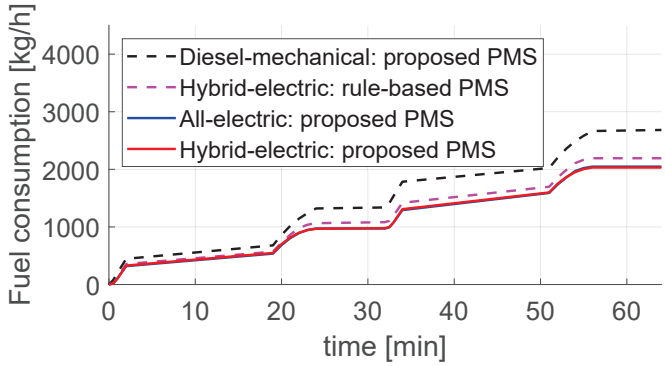

(f) Fuel consumption

Fig. 4: Simulation results for a *hybrid-electric* ferry with 300 kWh battery, C-rate (discharge/charge) 2.2C/1.6C, and 500 kW shore power.

with the benchmark *diesel-mechanical* architecture shown in Fig. 1c and the *all-electric* architecture shown in Fig. 1b. For a fair comparison among different architectures, the same major power system components are used in the simulation as given in Table II. Further, a rule-based power management given in [22] is also implemented as a *baseline* to compare the performance of the power management solution in the proposed design tool.

A. Power Breakdown

Fig. 3 shows the breakdown of power supply and demand with a 300 kWh battery and 500 kW shore power. The power supplies are plotted on the positive side of Y-axis and the power demands are plotted on the negative side. Fig. 3 shows that the proposed tool outputs a power allocation strategy which satisfies the power balance constraint for all the operational tasks, i.e., the total power supply equals the total power demand for all the tasks. Note that the dynamic power loss in the power system components is non-negligible as shown in Fig. 3.

B. Power Allocation Strategy

Figs. 4a–4d show initial and refined power allocation strategies and state-of-charge (SOC) for the vessel with 300 kWh battery and 500 kW shore power for a round-trip load profile. Fig. 4a shows the main engine power allocations for

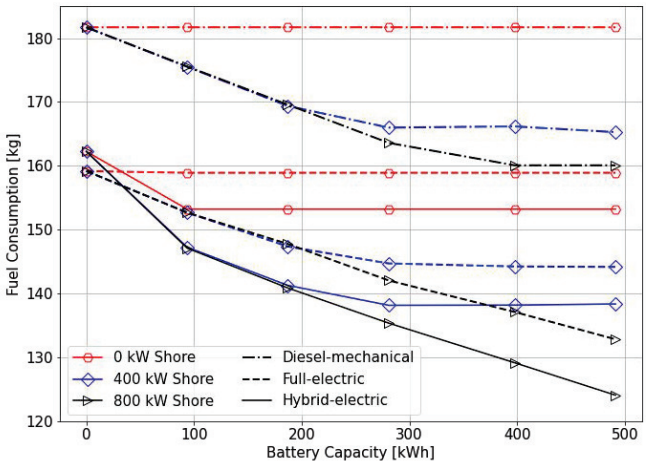

(a) Fuel consumption vs. battery size.

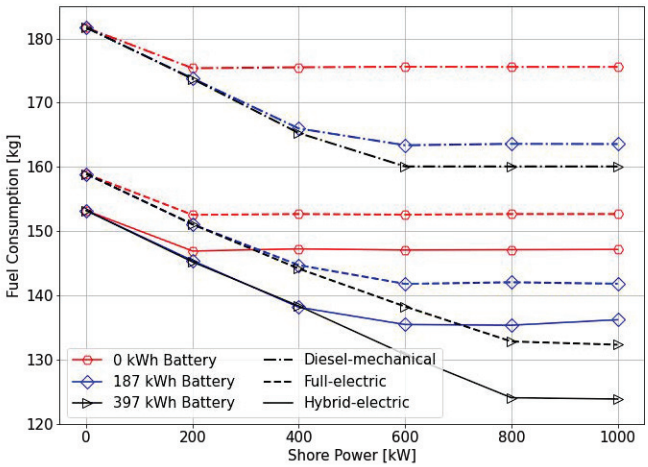

(b) Fuel consumption vs. shore power.

Fig. 5: Fuel consumption of ferry with respect to the battery size and shore power.

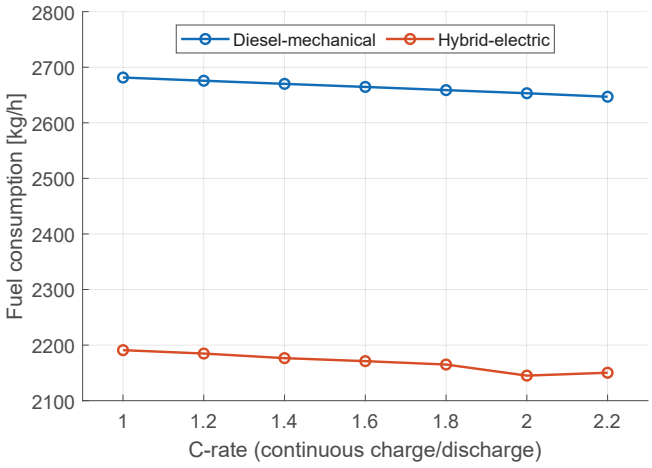

Fig. 6: Fuel consumption vs C-rate for 300 kWh battery and 1000kW shore power supply.

each task. The power allocation strategies for ME1-refined and ME2-refined are symmetric and optimal under the real-world constraints. Fig. 4b shows the auxiliary engine power allocations. Figs. 4a–4d demonstrate that the refinement step (Alg. 3) redistributes the power loads to the generators and the battery.

Fig. 4c shows the battery discharging or charging power with respect to operation time for each task. The corresponding battery SOC is displayed in Fig. 4d which shows that the battery is fully recharged back to 90% target at the end of the voyage (i.e., after harbor task). Because of the losses and specific fuel consumption are not linear, the refinement step significantly changes the discharging and charging amount. (See Fig. 4c–4d). This is reflected in the fuel consumption in each iteration plotted in Fig. 4e.

The cumulative fuel consumption comparison among different architectures is shown in Fig. 4f, which indicates that the traditional *diesel-mechanical* architecture consumes the most amount of fuel (2684 kg/hr), followed by the *all-electric* architecture in the second place (2047 kg/hr), and the *hybrid-electric* architecture consumes the least amount of fuel (2005 kg/hr). Since the main engine power generation cannot be optimized in *diesel-mechanical* architecture, it consumes the most fuel. Although *all-electric* architecture provides flexible power allocation, the two-step energy conversion, first from mechanical to electrical and then back to mechanical, consumes a significant portion of power. The *hybrid-electric* architecture provides power allocation flexibility where the propulsion power demand can be supplied mechanically or electrically or both mechanically and electrically, leading to the least amount of fuel consumed. Using *hybrid-electric* architecture reduces fuel consumption by 38.11% compared to the *diesel-mechanical* architecture and 2.05% compared to the *all-electric* architecture. Furthermore, the proposed two-step power management solution peforms better than the rule-based *baseline* solution, i.e., the fuel consumption decreases by 8.57% from 2193 kg/hr to 2005 kg/hr.

C. Battery Size and Shore Power Supply

Fig. 5 shows the fuel consumption against battery sizes under different shore power for the extracted average load profile in Fig. 2. The results show that the fuel consumption decreases with the increase in battery size until the recharging capacity is reached, where the fuel consumption remains constant. Fig. 5 shows that the maximum reducible fuel consumption is also affected by the shore power supply for charging, i.e., constrained by the shore power. The *diesel-mechanical* architecture supplies the propeller loads directly from the main engines, and only the hotel loads are optimized via the auxiliary engines (DGs) and the battery, showing the worst fuel consumption results. The *hybrid-electric* and *all-electric* architectures show significantly less fuel consumption than *diesel-mechanical* architecture since both architectures can allocate the entirety of the power demand optimally. The *hybrid-electric* architecture consumes less fuel than the *all-electric* architecture because *all-electric* needs two energy

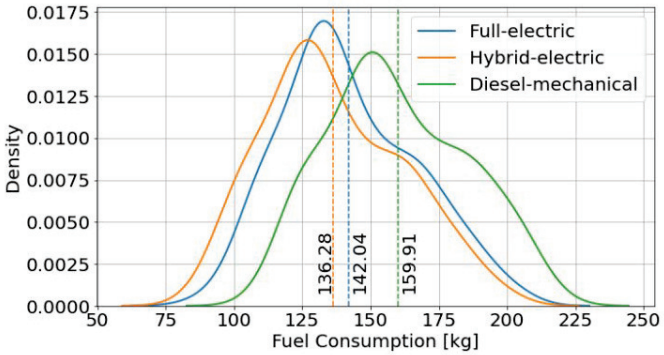

(a) p.d.f. of fuel consumption for 150 round trips

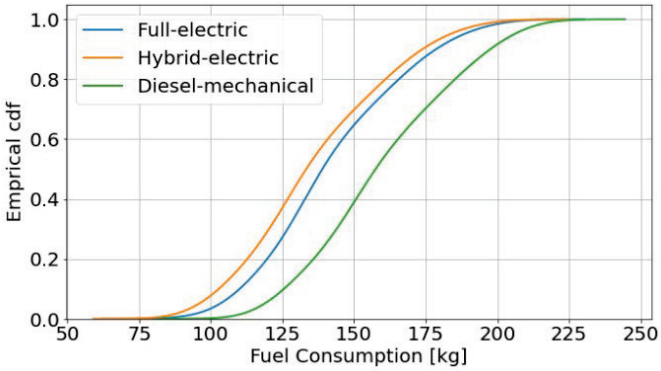

(b) c.d.f. of fuel consumption for 150 round trips

Fig. 7: Fuel consumption comparison for 150 round trips, 350 kWh battery, 500 kW shore supply, and 10 minutes harbor time.

conversions for propulsion power: mechanical-to-electrical and electrical-to-mechanical. These results clearly show the importance of charging infrastructure for electric vessels as in the case of the electric car industry.

D. Battery Charging and Discharging Rate

An experiment is run to test the effect of C-rate on the reduction of fuel consumption. Without loss of generality, the C-rate is set the same for discharging and charging for this experiment. For this experiment the shore power is set to 1000 kW so that the fuel consumption performance is not constrained by the available shore power. Fig. 6 shows the fuel consumption vs. different C-rate values. All cases show reduction of fuel consumption when increasing C-rate. These results imply that as the battery technology progress, the reduction in fuel consumption will continue and the vessel fully powered by *batteries* can be designed.

E. Architecture Comparison

Extensive simulations are run on each individual round-trip [22] to compare the fuel consumption. The p.d.f. and c.d.f. of the fuel consumption results are shown in Fig. 7. The results show that *hybrid-electric* performs better for high power demand trips because *all-electric* needs two energy conversions: mechanical-to-electrical and electrical-to-mechanical. Hence, there are more losses when the load demand is high. Performing the z-test on the average fuel consumption values gains a p-value of 0.0441, which is statistically significant. Hence, on average, the fuel consumption of *hybrid-electric* is lower than *all-electric*.

VI. Conclusion

This paper proposes a design tool to fill the industry application requirement. First, the power system components are modeled using the non-linear loss functions to reflect real-world mechanical and electrical engineering constraints. Next, a mixed-integer non-linear programming (MINLP) problem is formulated with *power balance* and *energy balance* constraints, which is decomposed into two tractable sub-problems: the battery discharging and charging sub-problem **(P1)** to guarantee *energy balance* and the generator and shore power allocation sub-problem **(P2)** to minimize the fuel consumption. The proposed solution to the MINLP problem is composed of two steps: *initialization* and *refinement*. Based on the boundary conditions, the *initialization* step outputs a feasible solution that satisfies the *power balance* and *energy balance* constraints, and the *refinement* step refines the initial output and converges to the optimum. The simulation results show that the proposed simulation tool can output an optimal power allocation strategy that fully recharges the battery to the target 90% SOC. In addition, the simulation results show that the *hybrid-electric* architecture leads to lower fuel cost compared to the *diesel-mechanical* and the *all-electric* architecture. Moreover, the proposed two-step power management solution outperforms the *rule-based baseline* solution. Furthermore, the battery sizing simulation results highlight the need to develop harbor charging infrastructure for electric vessels. The proposed tool will be extended to handle real-time power management with uncertainty, and new application domains will be explored.

Acknowledgment

The research, undertaken in the Rolls-Royce Corporate Lab @ Nanyang Technological University, is supported by the Singapore Government (Industry Alignment fund IAF-ICP Grant - I1801E0033). We thank E. Skjong for providing the dataset for our experiments.

References

[1] *Review of Maritime Transport 2019*. United Nations, Jan. 2020. [Online]. Available: https://www.ebook.de/de/product/38554088/review_of_maritime_transport_2019.html

[2] "World trade statistical review 2019," World Trade Organization, Tech. Rep., Nov. 2019. [Online]. Available: https://www.wto.org/english/res_e/statis_e/wts2019_e/wts19_toc_e.htm

[3] "Decarbonizingmaritime transport: Pathways to zero-carbon shipping by 2035," International Transport Forum, Tech. Rep., Mar. 2018. [Online]. Available: https://www.itf-oecd.org/decarbonising-maritime-transport

[4] L. Goldie-Scot, "A behind the scenes take on lithium-ion battery prices," Bloomberg NEF, Tech. Rep., Mar. 2019. [Online]. Available: https://about.bnef.com/blog/behind-scenes-take-lithium-ion-battery-prices/

[5] J. E. Harlow, X. Ma, J. Li, E. Logan, Y. Liu, N. Zhang, L. Ma, S. L. Glazier, M. M. E. Cormier, M. Genovese, S. Buteau, A. Cameron, J. E. Stark, and J. R. Dahn, "A wide range of testing results on an excellent lithium-ion cell chemistry to be used as benchmarks for new battery technologies," *Journal of The Electrochemical Society*, vol. 166, no. 13, pp. A3031–A3044, 2019.

[6] Y. Miao, P. Hynan, A. von Jouanne, and A. Yokochi, "Current li-ion battery technologies in electric vehicles and opportunities for advancements," *Energies*, vol. 12, no. 6, p. 1074, mar 2019.

[7] V. Smil, "Electric container ships are stuck on the horizon," IEEE Spectrum, Tech. Rep., Feb. 2019. [Online]. Available: https://spectrum.ieee.org/transportation/marine/electric-container-ships-are-stuck-on-the-horizon

[8] [Online]. Available: https://interferry.com/ferry-industry-facts/

[9] "What's driving the global ferry industry?" [website], 2018. [Online]. Available: https://www.ship-technology.com/features/whats-driving-global-ferry-industry

[10] "GT-Suite." [Online]. Available: https://www.gtisoft.com/gt-suite/gt-suite-overview/

[11] J. S. Thongam, M. Tarbouchi, A. F. Okou, D. Bouchard, and R. Beguenane, "All-electric ships – a review of the present state of the art," in *2013 Eighth International Conference and Exhibition on Ecological Vehicles and Renewable Energies (EVER)*. IEEE, mar 2013.

[12] T. J. McCoy, "Electric ships past, present, and future [technology leaders]," *IEEE Electrific. Mag.*, vol. 3, no. 2, pp. 4–11, jun 2015.

[13] F. D. Kanellos, G. J. Tsekouras, and N. D. Hatziargyriou, "Optimal demand-side management and power generation scheduling in an all-electric ship," *IEEE Trans. Sustain. Energy*, vol. 5, no. 4, pp. 1166–1175, oct 2014.

[14] F. D. Kanellos, "Optimal power management with GHG emissions limitation in all-electric ship power systems comprising energy storage systems," *IEEE Trans. Power Syst.*, vol. 29, no. 1, pp. 330–339, jan 2014.

[15] F. D. Kanellos, A. Anvari-Moghaddam, and J. M. Guerrero, "A cost-effective and emission-aware power management system for ships with integrated full electric propulsion," *Electric Power Systems Research*, vol. 150, pp. 63–75, sep 2017.

[16] E. Sciberras and R. Norman, "Multi-objective design of a hybrid propulsion system for marine vessels," *IET Electrical Systems in Transportation*, vol. 2, no. 3, p. 148, 2012.

[17] E. A. Sciberras, B. Zahawi, D. J. Atkinson, A. Breijs, and J. H. van Vugt, "Managing shipboard energy: A stochastic approach special issue on marine systems electrification," *IEEE Trans. Transport. Electrific.*, vol. 2, no. 4, pp. 538–546, dec 2016.

[18] C. Shang, D. Srinivasan, and T. Reindl, "NSGA-II for joint generation and voyage scheduling of an all-electric ship," in *2016 IEEE Congress on Evolutionary Computation (CEC)*. IEEE, jul 2016.

[19] ——, "Economic and environmental generation and voyage scheduling of all-electric ships," *IEEE Trans. Power Syst.*, vol. 31, no. 5, pp. 4087–4096, sep 2016.

[20] S. Fang, H. Cheng, and C. Zhang, "Joint generation and voyage scheduling for photovoltaic integrated all-electric ships," *The Journal of Engineering*, vol. 2019, no. 18, pp. 5085–5089, jul 2019.

[21] S. Fang, Y. Xu, Z. Li, T. Zhao, and H. Wang, "Two-step multi-objective management of hybrid energy storage system in all-electric ship microgrids," *IEEE Trans. Veh. Technol.*, vol. 68, no. 4, pp. 3361–3373, apr 2019.

[22] E. Skjong, T. A. Johansen, M. Molinas, and A. J. Sorensen, "Approaches to economic energy management in diesel–electric marine vessels," *IEEE Trans. Transport. Electrific.*, vol. 3, no. 1, pp. 22–35, mar 2017.

[23] A. G. Sarigiannidis, E. Chatzinikolaou, C. Patsios, and A. G. Kladas, "Shaft generator system design and ship operation improvement involving SFOC minimization, electric grid conditioning, and auxiliary propulsion," *IEEE Trans. Transport. Electrific.*, vol. 2, no. 4, pp. 558–569, dec 2016.

[24] E. K. Dedes, D. A. Hudson, and S. R. Turnock, "Assessing the potential of hybrid energy technology to reduce exhaust emissions from global shipping," *Energy Policy*, vol. 40, pp. 204–218, jan 2012.

[25] C. Yan, G. K. Venayagamoorthy, and K. A. Corzine, "Optimal location and sizing of energy storage modules for a smart electric ship power system," in *2011 IEEE Symposium on Computational Intelligence Applications In Smart Grid (CIASG)*. IEEE, apr 2011.

[26] S. Mashayekh, Z. Wang, L. Qi, J. Lindtjorn, and T. Myklebust, "Optimum sizing of energy storage for an electric ferry ship," in *2012 IEEE Power and Energy Society General Meeting*. IEEE, jul 2012.

[27] A. Boveri, F. Silvestro, M. Molinas, and E. Skjong, "Optimal sizing of energy storage systems for shipboard applications," *IEEE Trans. Energy Convers.*, vol. 34, no. 2, pp. 801–811, jun 2019.

[28] S. Boyd and L. Vandenberghe, *Convex Optimization*. New York, NY: Cambridge University Press, 2004. [Online]. Available: http://stanford.edu/~boyd/cvxbook/

[29] R. J. Vanderbei and D. F. Shanno, "An interior-point algorithm for nonconvex nonlinear programming," *Computational Optimization and Applications*, vol. 13, no. 1/3, pp. 231–252, 1999.

[30] "Corvus dolphin energy." [Online]. Available: https://corvusenergy.com/products/corvus-dolphin-energy/

Thant Zin Oo (M'18) received the B.Eng. degree in electrical systems and electronics from Myanmar Maritime University, Thanlyin, Myanmar, in 2008, the B.S. degree in computing and information systems from London Metropolitan University, U.K., in 2008, and the Ph.D. degree in computer science and engineering from Kyung Hee University, South Korea, in 2017. He is currently working as a research fellow at Nanyang Technological University, Singapore. His research interests include sustainable energy, power systems, wireless communications, cloud computing, optimization techniques, and AI.

Yan Ren received the B.Eng. degree in intelligence science and technology in 2011, the Ph.D. degree in circuit and system in 2018 from Xidian University, Xi'an, China. She is now a research fellow in Nanyang Technological University, Singapore. Her research interests include optimization-base power management, image object detection and instance segmentation.

Adams Wai-Kin Kong received the Ph.D. degree from the University of Waterloo, Canada. Currently, he is an associate professor at the Nanyang Technological University, Singapore. His research interests include pattern recognition and image processing.

Yi Wang received his Ph.D. degree in Computer Science and Engineering from the Hong Kong University of Science and Technology in 2009. He is currently an AI technologist with Central Technology and Strategy, Rolls-Royce Singapore. His research interest lies in automated reasoning and decision making and AI for engineering.

Xiong Liu (S'09–M'14–SM'19) received the B.E.and M.Sc. degrees in electrical engineering from Huazhong University of Science and Technology, Wuhan, China, in 2006 and 2008, respectively, and the Ph.D. degree from the School of Electrical and Electronic Engineering, Nanyang Technological University, Singapore in 2013. From July to November 2008, he was an Engineer with Shenzhen Nanrui Technologies Company Ltd., Shenzhen, China. From September 2011 to January 2012, he was a Visiting Scholar with the Department of Energy Technology, Aalborg University, Aalborg East, Denmark. From April 2012 to December 2013, he was a Researcher with the Energy Research Institute, Nanyang Technological University. From December 2013 to July 2020, he worked as a Principal Technologist in Rolls-Royce Electrical, Rolls-Royce Singapore Pte. Ltd., Singapore. He is currently an Associate Professor with the Energy Electricity Research Center, International Energy College, Jinan University, Zhuhai, China. His research interests include power electronics, motor drive, and electrical/hybrid propulsion systems for marine and aerospace. Dr. Liu was the recipient of the Best Paper Award at the IEEE International Power Electronics and Motion Control Conference-Energy Conversion Congress and Exposition Asia in 2012.